

Catalytic selective oxidation of isobutane over
 $\text{Cs}_x(\text{NH}_4)_{3-x}\text{HPMo}_{11}\text{VO}_{40}$ mixed salts†Cite this: *Catal. Sci. Technol.*, 2014,
4, 2938Fangli Jing,^{ab} Benjamin Katryniok,^{abc} Franck Dumeignil,^{abde} Elisabeth Bordes-Richard^{abf}
and Sébastien Paul^{*abc}

A series of mixed Keggin-type heteropolysalts $\text{Cs}_x(\text{NH}_4)_{3-x}\text{HPMo}_{11}\text{VO}_{40}$ with various ammonia/caesium ratios was prepared by the precipitation method and characterized by TGA, N_2 adsorption/desorption, XRD, FT-IR, and NH_3 -TPD techniques. Correlations between the ammonia/caesium ratio and the specific surface area, as well as with the total number of acid sites, were established. Furthermore, the introduction of Cs to the catalytic formulation was beneficial to the stabilization of the Keggin structure and helped limiting the elimination of the V atoms from the primary structure. The as-prepared samples were applied in the catalytic selective oxidation of isobutane at 340 °C under atmospheric pressure. The best results were obtained over $\text{Cs}_{1.7}(\text{NH}_4)_{1.3}\text{HPMo}_{11}\text{VO}_{40}$ with an isobutane conversion of 9.6% and a total selectivity to valuable products (methacrylic acid and methacrolein) of 57.1%. This was explained by the well-balanced acidity and specific surface of this catalyst, promoting the C–H bond activation (adequate acid properties) over a large number of accessible active sites (high acid sites density).

Received 21st April 2014,
Accepted 14th May 2014

DOI: 10.1039/c4cy00518j

www.rsc.org/catalysis

1. Introduction

The development of an efficient catalyst for the selective oxidation of isobutane would provide a very interesting shortcut for the production of methacrolein (MAC) and methacrylic acid (MAA), which could be further used in the synthesis of polymethyl methacrylate polymer (PMMA). The conventional process for producing PMMA is based on the acetone-cyanohydrin (ACH) route,¹ which has two main drawbacks: the use of a highly toxic raw material – namely, hydrogen cyanide – and the production of large amounts of contaminated by-products (mainly ammonium bisulphate). In comparison with the traditional techniques, the advantages of the direct catalytic isobutane selective oxidation are obvious: simplicity of the process, low cost of the raw materials, environmental friendliness and, last but not least, less by-products generation. Bifunctional catalysts possessing simultaneously acid and redox properties are necessary for catalysing such a

reaction. Hereby, the acidity plays an important role in activating the C–H bond, and the redox properties are responsible for the oxygen insertion in the hydrocarbon skeleton to generate the carboxylic acid function.

In a previous study, we demonstrated that $(\text{NH}_4)_3\text{HPMo}_{11}\text{VO}_{40}$ (APMV) supported on $\text{Cs}_3\text{PMo}_{12}\text{O}_{40}$ (CPM) enables high catalytic performance in the selective oxidation of isobutane.^{2,3} Thus came the idea of studying the $\text{Cs}^+/\text{NH}_4^+$ mixed salts of 1-vanado-11-molybdophosphoric acid for the selective oxidation of isobutane. Various studies on (mixed) salts of heteropolycompounds such as, for instance, $(\text{NH}_4)_3\text{PW}_{12}\text{O}_{40}$,⁴ $\text{Cs}_x\text{H}_{3-x}\text{PW}_{12}\text{O}_{40}$,⁵ $\text{Cs}_x(\text{NH}_4)_{3-x}\text{PW}_{12}\text{O}_{40}$ (ref. 6) or $\text{Cs}_x(\text{NH}_4)_{3-x}\text{PM}_{12}\text{O}_{40}$ (ref. 7,8) have already been published, but these solids were not used as catalysts for the isobutane selective oxidation to methacrolein and/or methacrylic acid. Herein, we report the preparation and the application of $\text{Cs}^+/\text{NH}_4^+$ mixed acid salts of 1-vanado-11-molybdophosphoric corresponding to the formula $\text{Cs}_x(\text{NH}_4)_{3-x}\text{HPMo}_{11}\text{VO}_{40}$, and using various ratios between caesium and ammonium cations with $x = 3, 2.5, 1.7, 1.5, 0.5$ and 0. Next to the influence of the counter-cations ratio on the catalytic performances, the effect of the composition on the structural, the textural and the acidic properties of the solids was also studied.

2. Experimental

2.1 Catalysts preparation

The synthesis of the parent heteropolyacid ($\text{H}_4\text{PMo}_{11}\text{VO}_{40}$) was performed as reported elsewhere.⁹ The mixed salts

^a Univ. Lille Nord de France, F-59000, Lille, France^b Unité de Catalyse et de Chimie du Solide, UCCS (UMR CNRS 8181), Cité Scientifique, F-59650, Villeneuve d'Ascq, France^c Ecole Centrale de Lille, ECLille, F-59655 Villeneuve d'Ascq, France.

E-mail: sebastien.paul@ec-lille.fr; Fax: +33 3 20 33 54 99; Tel: +33 3 20 33 54 57

^d Université Lille 1 Sciences et Technologies, USTL, F-59652 Villeneuve d'Ascq, France^e Institut Universitaire de France, Maison des Universités, 103 Bd St-Michel, Paris, 75005, France^f Ecole Nationale Supérieure de Chimie de Lille, ENSCL, F-59659 Villeneuve d'Ascq, France† Electronic supplementary information (ESI) available: Raman spectra, XRD diffractograms, N_2 adsorption–desorption, NH_3 -TPD. See DOI: 10.1039/c4cy00518j

$\text{Cs}_x(\text{NH}_4)_{3-x}\text{HPMo}_{11}\text{VO}_{40}$ ($x = 3, 2.5, 1.7, 1.5, 0.5$ and 0) were prepared by a precipitation method. In a typical synthesis procedure, the appropriate amount of $\text{H}_4\text{PMo}_{11}\text{VO}_{40}$ acid was dissolved under stirring in deionized water to obtain a 0.05 M solution at $45 \text{ }^\circ\text{C}$. Then, solutions of Cs_2CO_3 (0.05 M) and of NH_4NO_3 (0.05 M) were added using a pump with a constant flowrate of 2 mL min^{-1} under vigorous stirring. The reaction mixture was kept as such for 18 h for ageing, and, then, the so-obtained precipitate was recovered by evaporating the solvent at $70 \text{ }^\circ\text{C}$ under reduced pressure. Afterwards, the solid was dried at $70 \text{ }^\circ\text{C}$ in an oven for another 24 h . The final catalysts were obtained after thermal treatment at $350 \text{ }^\circ\text{C}$ for 3 h under static air to decompose the nitrate and carbonate precursors in order to obtain the mixed salts. The samples were denoted as $\text{Cs}_x(\text{NH}_4)_{3-x}\text{H}$ ($x = 3, 2.5, 1.7, 1.5, 0.5$ and 0) according to the theoretical catalyst composition. In the case of $x = 0$, the sample corresponds to the ammonium acidic salt of the phospho-vanado-molybdic acid, which is denoted APMV in the following.

2.2 Catalysts characterization

Thermogravimetric analyses (TGA) were performed on fresh catalysts using a TA instruments (Model 2960 SDT, V3.0F). The catalysts were heated from room temperature to $700 \text{ }^\circ\text{C}$ with an increasing rate of $3 \text{ }^\circ\text{C min}^{-1}$ under air flow.

The textural properties of the calcined catalysts were determined by the N_2 physisorption/desorption technique, using a Micromeritics ASAP 2010 analyser at the liquid nitrogen temperature. The specific surface area (S_{BET}) was calculated using the BET method.¹⁰ The total pore volume (V_{p}) was determined using the value observed at the relative pressure (P/P_0) of 0.995 . The samples were outgassed at $150 \text{ }^\circ\text{C}$ for 3 h prior to analysis.

Infrared spectra (FT-IR) were recorded on a Thermo Nicolet 480 equipped with a MCT detector. The samples ($1 \text{ wt.}\%$) were pressed to form KBr pellets for analysis, and the spectra were recorded from 400 to 4000 cm^{-1} with a spectral resolution of 4 cm^{-1} and 256 scans.

The crystalline structure of the catalysts was resolved by X-ray diffraction (XRD) technique on a Bruker D8 Advance diffractometer, using the $\text{CuK}\alpha$ radiation ($\lambda = 1.5506 \text{ \AA}$) as X-ray source. A range from $10^\circ < 2\theta < 80^\circ$ was scanned with a step of $0.02^\circ \text{ s}^{-1}$ and 2 s of acquisition time. The crystallite size was estimated by the Debye-Scherrer's equation, namely $L = 0.89\lambda/\beta(\theta)\cos\theta$, where L is the crystallite size, λ is the wavelength of the radiation used, θ is the Bragg diffraction angle and $\beta(\theta)$ is the full width at half maximum (FWHM).^{11,12}

Ammonia temperature-programmed desorption (NH_3 -TPD) was employed in order to determine the amount and the strength of the acid sites over the solids. A typical acquisition was carried out as follows: 50 mg of catalyst were pre-treated in a He flow (30 mL min^{-1}) at $250 \text{ }^\circ\text{C}$ for 2 h in order to remove the physisorbed and the crystal water. Then, NH_3 was absorbed at the surface by pulsed injections at $130 \text{ }^\circ\text{C}$ until

saturation (evaluated from the thermal conductivity detector – TCD – signal). The TPD profiles were monitored by a TCD and recorded from 130 to $700 \text{ }^\circ\text{C}$ at the heating rate of $10 \text{ }^\circ\text{C min}^{-1}$. The effluent gas was identified by a mass spectrometer.

2.3 Catalytic selective oxidation of isobutane

The catalytic performances in the selective oxidation of isobutane to methacrolein and methacrylic acid were evaluated in a fixed-bed reactor at $340 \text{ }^\circ\text{C}$ under atmospheric pressure. 0.8 g of catalyst diluted in 0.8 – 1.6 g SiC (0.21 mm particle size) were loaded in the middle of the reactor. The reactants [27% isobutane, 13.5% O_2 , 10% H_2O and 49.5% He (mol.%)] were fed at a constant total flow-rate of 10 mL min^{-1} . All the products – except water – were analysed by online gas chromatography (GC). The incondensable compounds such as CO, CO_2 , O_2 and isobutane (IBAN) were analysed by a GC equipped with a TCD and 2 packed columns in series (Porapak Q, 3.2 mm diameter, 3 m length; molecular sieve 13X, 3.2 mm diameter, 3 m length). The less volatile products like methacrolein (MAC), methacrylic acid (MAA), acetic acid (AA) and acrylic acid (ACA) were analysed by a GC equipped with a flame ionization detector (FID) and an Alltech EC1000 semi-capillary column (30 m length, 0.53 mm diameter, $1.2 \text{ }\mu\text{m}$ film width). The reaction data were obtained after 18 h under stream, which corresponds to steady state conditions (typically reached within 2 h).

3. Results and discussion

3.1 Thermal stability

The thermal analyses of two samples, one without NH_4^+ cations ($x = 3$) and another one with NH_4^+ cations ($x = 1.7$, taken as an example) were carried out under air flow to study the structural evolution during the calcination (Fig. 1). A continuous weight loss was observed from the TG curves (solid lines) from the starting temperature to $450 \text{ }^\circ\text{C}$ for both samples. A more precise picture can be obtained from the DTG curves (dash lines). The initial stage between 100 – $205 \text{ }^\circ\text{C}$ was ascribed to the removal of physisorbed and crystal water.

Afterwards, a broad peak between $175 \text{ }^\circ\text{C}$ and $500 \text{ }^\circ\text{C}$ for the $\text{Cs}_3(\text{NH}_4)_0\text{H}$ sample was assigned to the loss of one proton as constitution water.¹³ The calculated weight loss for this step is 0.41% , which is close to the theoretical value (0.48%). In the case of $\text{Cs}_{1.7}(\text{NH}_4)_{1.3}\text{H}$, a multi-step decomposition between $205 \text{ }^\circ\text{C}$ and $430 \text{ }^\circ\text{C}$ was observed. As already reported,² the total removal of ammonium cations consists of 2 steps: the release of NH_3 to give the residual acidic protons, and subsequent loss of the residual protons as constitution water. The weight loss of 1.86% observed on the TG curve was in rather good agreement with the theoretical value (2.04%), which suggests almost complete loss of proton and ammonium cations. For both samples, Keggin type compounds with oxygen vacancies were generated after the elimination of constitutional water as it is well-known from the literature.¹⁴ Finally, the Keggin structure collapsed to form the simple P_2O_5 , V_2O_5 and MoO_3 oxides at $630 \text{ }^\circ\text{C}$ for the

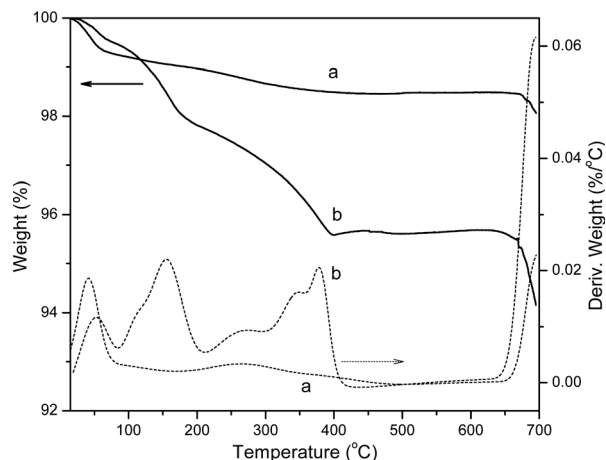


Fig. 1 Thermogravimetric (TG, solid lines) and derivative thermogravimetric analysis (DTG, dash lines) [a: $\text{Cs}_3(\text{NH}_4)_0\text{H}$; b: $\text{Cs}_{1.7}(\text{NH}_4)_{1.3}\text{H}$].

$\text{Cs}_{1.7}(\text{NH}_4)_{1.3}\text{H}$ sample, and at 654 °C for the $\text{Cs}_3(\text{NH}_4)_0\text{H}$ sample. Simultaneously, the P_2O_5 began to sublime, resulting in further weight loss. From these results, it can be deduced that the active phase can partially release NH_3 at the studied reaction temperature (namely 340 °C), leading to a protonated heteropolycompound species.

3.2 Structural features

The structural features of the catalysts were determined by FT-IR spectroscopy and X-ray diffraction. The FT-IR spectra of the calcined catalysts are reported in Fig. 2. The vibration bands at 1061, 963, 865 and 788 cm^{-1} are attributed to the asymmetric stretching of heteroatom-oxygen ($\nu_{\text{as}} \text{P-O}$), the peripheral metal atoms-terminal oxygen ($\nu_{\text{as}} \text{M=O}_t$), the stretching mode of inter- and intra-octahedral bridges ($\nu_{\text{as}} \text{M-O}_b\text{-M}$ and $\nu_{\text{as}} \text{M-O}_c\text{-M}$), respectively.^{15–17} In addition, for the $\text{Cs}_3(\text{NH}_4)_0\text{H}$ (Fig. 2a) and $\text{Cs}_{2.5}(\text{NH}_4)_{0.5}\text{H}$ samples (Fig. 2b), two shoulders can be clearly observed at 1080 and

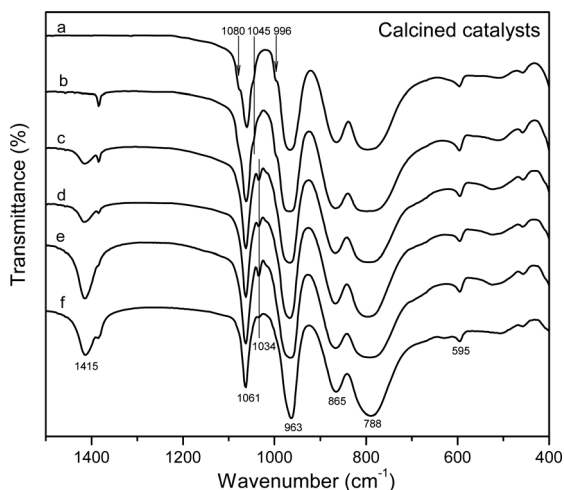


Fig. 2 FT-IR spectra of the calcined samples [a: $\text{Cs}_3(\text{NH}_4)_0\text{H}$, b: $\text{Cs}_{2.5}(\text{NH}_4)_{0.5}\text{H}$, c: $\text{Cs}_{1.7}(\text{NH}_4)_{1.3}\text{H}$, d: $\text{Cs}_{1.5}(\text{NH}_4)_{1.5}\text{H}$, e: $\text{Cs}_{0.5}(\text{NH}_4)_{2.5}\text{H}$, f: APMV].

996 cm^{-1} , which are considered as characteristic of the substitution of one Mo atom by one V atom in the Keggin anion $\text{PMo}_{12}\text{O}_{40}^{3-}$.¹⁸ In fact, the exchange of one Mo by one V reduces the symmetry, leading to a weak distortion of the PO_4 tetrahedron. A third shoulder at 1045 cm^{-1} also present on both samples is assigned to the asymmetric stretching mode of P-O. The other samples with lower Cs contents (Fig. 2c–f) do not exhibit these three shoulders observed for $\text{Cs}_3(\text{NH}_4)_0\text{H}$ and $\text{Cs}_{2.5}(\text{NH}_4)_{0.5}\text{H}$. Instead, a weak peak appears at 1034 cm^{-1} , which is assigned to the $\nu \text{V=O}$ band of V_2O_5 .¹⁹ The characteristic band of N-H can be observed at 1415 cm^{-1} in the samples containing NH_4^+ (Fig. 2b–f) except for $\text{Cs}_{2.5}(\text{NH}_4)_{0.5}\text{H}$, in which the NH_4^+ may have been removed as NH_3 during the thermal treatment. The band at lower wavenumber of 595 cm^{-1} , observed on all the samples, can be attributed to MoO_3 ,²⁰ while the band at 1384 cm^{-1} , observed on all the N-containing samples, is related to the presence of residual NO_3^- .

These results indicate that the structure of the synthesized solids significantly depends on the number of Cs atoms. For a high Cs loading (namely for $x = 3$ and 2.5), the structural features due to V-substituted Keggin anions are still clearly visible. When the Cs atoms number progressively decreases to finally reach zero for APMV, the aforementioned structural features concomitantly disappear to the profit of new features from V_2O_5 , suggesting the elimination of V from the primary structure. At the same time, the detection of MoO_3 by IR suggests a partial decomposition during calcination. This latter interpretation was also confirmed by Raman analysis (Fig. S1†).

Except for $\text{Cs}_3(\text{NH}_4)_0\text{H}$ the FT-IR spectra of the spent catalysts exhibit the nearly the same features as those of the fresh samples but an additional band at 629 cm^{-1} attributed to MoO_2 (Fig. 3; S2† for full-scale spectra). It was explained by the fact that the MoO_3 species issued from the partial decomposition of Keggin anions (band at 595 cm^{-1}) were partially reduced to MoO_2 by isobutane under reaction conditions.^{7,21} Since the intensity of the 629 cm^{-1} band increased with the decrease in the Cs loading, this supports the hypothesis that the introduction of Cs stabilizes the Keggin structure under the reaction conditions.

X-Ray diffraction was used to determine the crystalline phases present in the $\text{Cs}_x(\text{NH}_4)_{3-x}\text{H}$ ($x = 0\text{--}3$) mixed salts samples. The patterns of the calcined and used catalysts are presented in Fig. 4 and S3†, respectively. All the samples exhibit three strong diffraction peaks at $2\theta = 26.4^\circ$, 10.6° and 36.0° , which are characteristic of the Keggin structure.²² When introducing Cs into the catalysts, the patterns show the trend to be shifted to lower angles, which is characteristic of an increase in the d -spacing according to the Bragg's law. In fact, when NH_4^+ cations are partially substituted by Cs^+ cations, the inter-planar spacing is expanded, simply because Cs^+ has a larger ionic radius than NH_4^+ . Thus, the d -spacing of plane (222) for the calcined samples increased from 0.3377 nm for the Cs-free APMV sample to 0.3416 nm for the $\text{Cs}_{2.5}(\text{NH}_4)_{0.5}\text{H}$ sample (Table 1). On the other hand, a slight decrease in the

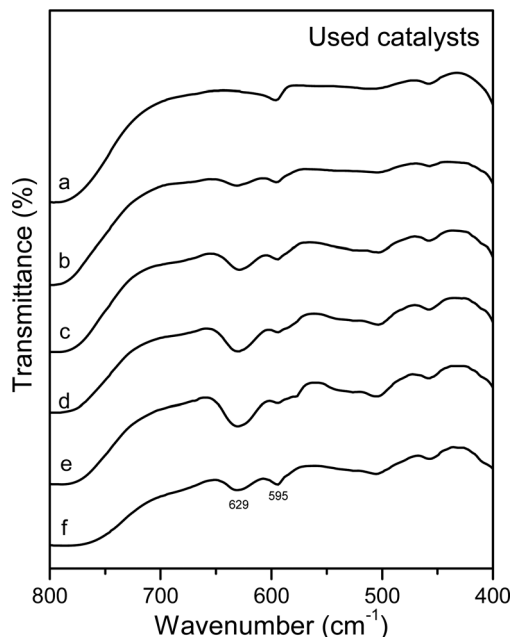


Fig. 3 FT-IR spectra of the spent catalysts [a: $\text{Cs}_3(\text{NH}_4)_0\text{H}$, b: $\text{Cs}_{2.5}(\text{NH}_4)_{0.5}\text{H}$, c: $\text{Cs}_{1.7}(\text{NH}_4)_{1.3}\text{H}$, d: $\text{Cs}_{1.5}(\text{NH}_4)_{1.5}\text{H}$, e: $\text{Cs}_{0.5}(\text{NH}_4)_{2.5}\text{H}$, f: APMV].

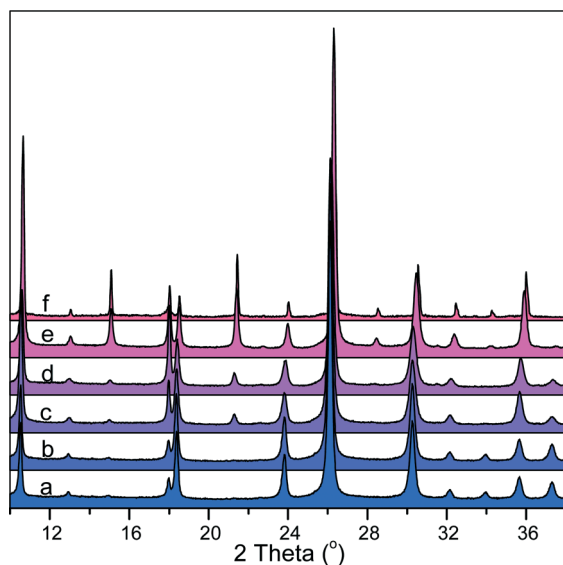


Fig. 4 XRD patterns of the different catalysts before reaction [a: $\text{Cs}_3(\text{NH}_4)_0\text{H}$, b: $\text{Cs}_{2.5}(\text{NH}_4)_{0.5}\text{H}$, c: $\text{Cs}_{1.7}(\text{NH}_4)_{1.3}\text{H}$, d: $\text{Cs}_{1.5}(\text{NH}_4)_{1.5}\text{H}$, e: $\text{Cs}_{0.5}(\text{NH}_4)_{2.5}\text{H}$, f: APMV]. The diffraction line observed at 18° is due to the Teflon holder.

d -spacing could be observed for the fully substituted sample $\text{Cs}_3(\text{NH}_4)_0\text{H}$. It is important to note that two diffraction peaks at $2\theta = 15.1^\circ$ and 21.4° only appear for the catalysts containing NH_4^+ . The intensities of these peaks weaken as the number of NH_4^+ cations decreases, and they are ultimately not detected at all over the $\text{Cs}_3(\text{NH}_4)_0\text{H}$ sample. Therefore, these two diffraction lines could be considered as characteristic of the presence of NH_4^+ cations-containing polyoxometalates.

In order to gain more information about the structural evolution of the catalysts during the reaction, the cell parameters a of the cubic phases were also calculated. We selected six diffraction planes including (110), (211), (310), (222), (400) and (332), which give the characteristic XRD lines of the Keggin type heteropolycompounds. The relationship between the cell parameter a and the Cs loading, represented by 'x' in the $\text{Cs}_x(\text{NH}_4)_{3-x}\text{HPMo}_{11}\text{VO}_{40}$ formula, is reported in Fig. 5. For the samples before reaction, a linear relationship between a and x is observed, meaning that the partial substitution of ammonia by caesium cations obeys the Vegard's law.

The cell parameter a changes irregularly after reaction, reflecting a complex structural evolution of the heteropolycompounds under the reaction conditions. However, a linear relationship is obtained for the Cs contained catalysts, and the observed evolution of the a parameter between the fresh and the used samples depends on the Cs loading. The catalyst with the lower Cs content [namely $\text{Cs}_{0.5}(\text{NH}_4)_{2.5}\text{H}$] shows an increase of the a value between the fresh and the spent sample (11.76 \AA vs. 11.74 \AA). In contrast, almost no change is observed for the $\text{Cs}_{1.5}(\text{NH}_4)_{1.5}\text{H}$ sample, with a a value around 11.79 \AA before and after reaction. In contrast, for the samples with the higher contents in Cs such as $\text{Cs}_{1.7}(\text{NH}_4)_{1.3}\text{H}$, $\text{Cs}_{2.5}(\text{NH}_4)_{0.5}\text{H}$ and $\text{Cs}_3(\text{NH}_4)_0\text{H}$, a is clearly lowered after reaction. It seems that these samples evolve towards the stable $\text{Cs}_4\text{PMo}_{11}\text{VO}_{40}$ phase, which exhibits a a value of 11.75 \AA (PDF#46-0481), but probably under a protonated form. It can be concluded combining TGA and FT-IR results that: i) the successive loss of ammonium cations and residual protons as NH_3 and water may take place under the reaction conditions; ii) the introduction of Cs in the catalysts stabilizes the V-containing Keggin structure, thus protecting V against the elimination from the primary structure. To this respect, we can remark that the a cell parameter observed for $\text{Cs}_{0.5}(\text{NH}_4)_{2.5}\text{H}$ is much closer to that of $\text{Cs}_4\text{PMo}_{11}\text{VO}_{40}$ than the other Cs-containing samples, as it exhibits a weaker ability to stabilize the structure. For the APMV Cs-free sample, the value decreases to 11.68 \AA after test, which is quite close to that of $(\text{NH}_4)_3\text{PMo}_{12}\text{O}_{40}$ ($a = 11.67 \text{ \AA}$, PDF#43-0315). This evidences the fact that in absence of caesium the V-containing Keggin structure cannot be stabilized.

Additionally, the influence of the Cs introduction on the crystallites size was also investigated. The crystallite size of the catalysts was estimated using the Debye-Shererr's equation from the values of the FWHM of the (110), (222) and (332) diffraction planes.^{5,12} The APMV sample showed the largest crystallite size ($>100 \text{ nm}$) under the calcined and the spent form. The introduction of caesium in the catalyst favoured the formation of crystallites with a smaller size, which is in agreement with the textural properties of the solids (*vide infra*). Furthermore, it was found that the crystallite size slightly increased after reaction, thus suggesting the sintering of the catalyst.

3.3 Textural properties of the calcined samples

The textural properties of the calcined samples including the specific surface area (S_{BET}), the total porous volume (V), and

Table 1 Average crystallite size & related parameters of the samples, as determined using XRD patterns

Sample	Before reaction		
	2θ for hkl (222)	$d(222)$, nm	Average crystallite size, nm
$\text{Cs}_0(\text{NH}_4)_3\text{H}$ (APMV)	26.37	0.3377	>100 (>100) ^a
$\text{Cs}_{0.5}(\text{NH}_4)_{2.5}\text{H}$	26.29	0.3387	45.7 (47.2)
$\text{Cs}_{1.5}(\text{NH}_4)_{1.5}\text{H}$	26.18	0.3400	39.4 (42.2)
$\text{Cs}_{1.7}(\text{NH}_4)_{1.3}\text{H}$	26.12	0.3408	38.8 (42.3)
$\text{Cs}_{2.5}(\text{NH}_4)_{0.5}\text{H}$	26.06	0.3416	36.9 (44.9)
$\text{Cs}_3(\text{NH}_4)_0\text{H}$	26.10	0.3411	41.9 (46.4)

The values $d(222)$ for $(\text{NH}_4)_3\text{PMo}_{12}\text{O}_{40}$ (PDF#43-0315), $\text{Cs}_3\text{PMo}_{11}\text{VO}_{40}$ (PDF#46-0481) and $\text{H}_4\text{PMo}_{11}\text{VO}_{40}$ (PDF#52-1117) are 0.3370, 0.3393 and 0.3377 nm, respectively.^a The values in parenthesis correspond to the spent catalysts.

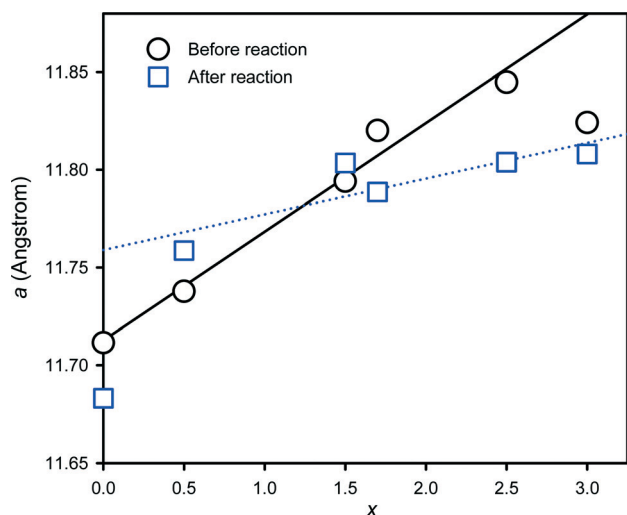


Fig. 5 Correlation between the cell parameter a and the x number of Cs atoms in the $\text{Cs}_x(\text{NH}_4)_{3-x}\text{HPMo}_{11}\text{VO}_{40}$ catalysts. The cell parameter a was calculated using the following formula: $a = d(hkl) \cdot \sqrt{(h^2 + k^2 + l^2)}$.

the average pore diameter (D) are reported in Table 2. The textural properties are strongly depending on the $\text{Cs}^+/\text{NH}_4^+$ ratio. The APMV sample – without Cs cations – shows a low S_{BET} ($3.5 \text{ m}^2 \text{ g}^{-1}$), which suggests the formation of a bulk, non-porous-like material. Upon progressive replacement of the NH_4^+ cations by Cs^+ cations, the surface area gradually increases. When the number of Cs cations (x) in the catalyst increases from 0.5 to 1.7, the specific surface area increases from 5.8 to $16.4 \text{ m}^2 \text{ g}^{-1}$. Then, the surface area reaches the maximum value of $87.6 \text{ m}^2 \text{ g}^{-1}$ when all NH_4^+ cations are substituted by Cs^+ cations [$\text{Cs}_3(\text{NH}_4)_0\text{H}$]. The correlation between the Cs content and the surface area is represented

Table 2 Textural properties of the calcined mixed salts samples

x	Sample	S_{BET} , $\text{m}^2 \text{ g}^{-1}$	V , $\text{cm}^3 \text{ g}^{-1}$	D , nm
0	$\text{Cs}_0(\text{NH}_4)_3\text{H}$ (APMV)	3.5	0.020	23.1
0.5	$\text{Cs}_{0.5}(\text{NH}_4)_{2.5}\text{H}$	5.8	0.014	11.1
1.5	$\text{Cs}_{1.5}(\text{NH}_4)_{1.5}\text{H}$	8.4	0.018	7.1
1.7	$\text{Cs}_{1.7}(\text{NH}_4)_{1.3}\text{H}$	16.4	0.033	6.5
2.5	$\text{Cs}_{2.5}(\text{NH}_4)_{0.5}\text{H}$	58.6	0.040	4.2
3.0	$\text{Cs}_3(\text{NH}_4)_0\text{H}$	87.6	0.035	4.5

in Fig. 6 (circles). The specific surface area of the catalyst increases linearly as the Cs number increases from 1.5 to 3.0. On the other hand, when the Cs number is as low as 0.5, the correlation does no longer fit. However, the value is still higher than that of the Cs-free sample, namely $\text{Cs}_0(\text{NH}_4)_3\text{H}$ (APMV). These results show that it is possible to increase the specific surface area of the solids by introducing some caesium cations in the catalysts formulation.

On the other hand, an inverse linear relationship is found between the average pore diameter (square symbols in Fig. 6) and the caesium content. Nevertheless, the BJH model evidences a rather broad pore size distribution (Fig. S4[†]). Only in the case of $\text{Cs}_{1.5}(\text{NH}_4)_{1.5}\text{H}$ and $\text{Cs}_{1.7}(\text{NH}_4)_{1.3}\text{H}$, a discrete distribution is observed with a maximum at 4 nm. This mesoporous feature is further underlined by the isotherms corresponding to an IUPAC type IV with a H3 hysteresis (Fig. S5[†]). On the other hand, no clear picture is obtained from the evolution of the total pore volume with the Cs content.

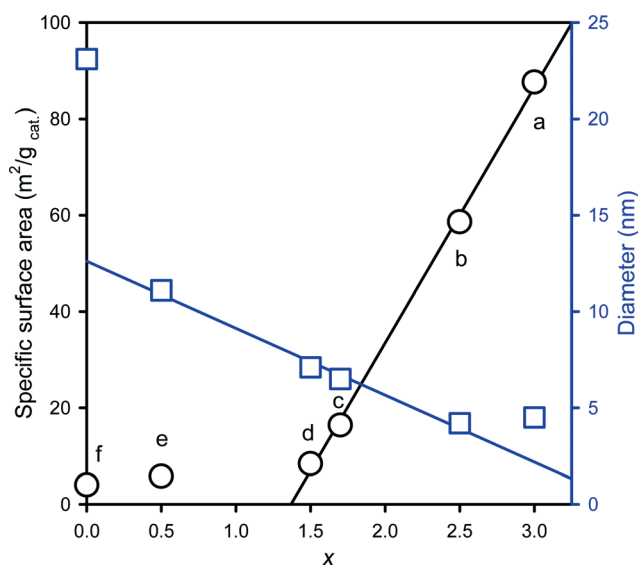


Fig. 6 Plots of surface area (circles) and pore diameter (squares) as a function of the Cs loading expressed as x in the $\text{Cs}_x(\text{NH}_4)_{3-x}\text{HPMo}_{11}\text{VO}_{40}$ calcined samples [a: $\text{Cs}_3(\text{NH}_4)_0\text{H}$, b: $\text{Cs}_{2.5}(\text{NH}_4)_{0.5}\text{H}$, c: $\text{Cs}_{1.7}(\text{NH}_4)_{1.3}\text{H}$, d: $\text{Cs}_{1.5}(\text{NH}_4)_{1.5}\text{H}$, e: $\text{Cs}_{0.5}(\text{NH}_4)_{2.5}\text{H}$, f: APMV].

3.4 Acid properties (NH₃-TPD)

The selective oxidation of isobutane to methacrolein and methacrylic acid is significantly impacted by the nature and the strength of the acid sites, which have to activate the C–H bond, promoting the conversion of MAC to MAA and driving the desorption of the formed acid products like MAA from the catalysts surface.^{23–25} Therefore, it is worth investigating the acidic properties of the prepared catalysts. The NH₃-TPD profiles were collected between 130 to 700 °C (Fig. S6†) and the amount of acidic sites was quantified by deconvolution/integration of the profiles (Table 3 and Fig. S8†). The amount of desorbed ammonia was corrected by the amount of ammonia yielding from the decomposition of the ammonium cations. The detailed method used is described elsewhere.² Three types of acidic sites with different strengths were defined, corresponding to weak sites in the 130–300 °C range, medium sites in the 300–450 °C range and strong acidic sites in the 450–560 °C range, respectively. Strong acidic sites are only observed for the catalyst having the lowest Cs content [Cs_{0.5}(NH₄)_{2.5}H] (1.16 mmol g_{cat.}⁻¹), this sample being also the catalyst exhibiting the largest total amount of acid sites of the series (1.84 mmol g_{cat.}⁻¹). The other samples only exhibit medium sites together with a very small amount of weak sites.

The amount of acid sites per mass of catalyst linearly increased when *x* decreased (Fig. 7). As the specific surface area also increased when *x* decreased (Table 2), the highest surface acidic sites density (317.55 μmol m_{cat.}⁻²) was accordingly observed over the Cs_{0.5}(NH₄)_{2.5}H catalyst.

3.5 Catalytic performance in the reaction of isobutane partial oxidation

The prepared catalysts were used to catalyse the selective oxidation of isobutane to MAC and MAA. The results are listed in Table 4. The Cs-free APMV exhibited rather low conversions in both oxygen and isobutane (10.4% and 2.0%, respectively). The introduction of Cs in the catalysts formulas dramatically affected both the conversion of reactants and the products distribution. Over the catalyst with the lowest Cs content, namely Cs_{0.5}(NH₄)_{2.5}H, the isobutane conversion is 4.1%, more than 2 times as high as that obtained over APMV, and the yield of the desired products (MAC + MAA) was more than tripled. With the increase in *x* up to 2.5, the maximum conversion of isobutane (9.9%) was achieved, and, simultaneously, full conversion of oxygen was observed.

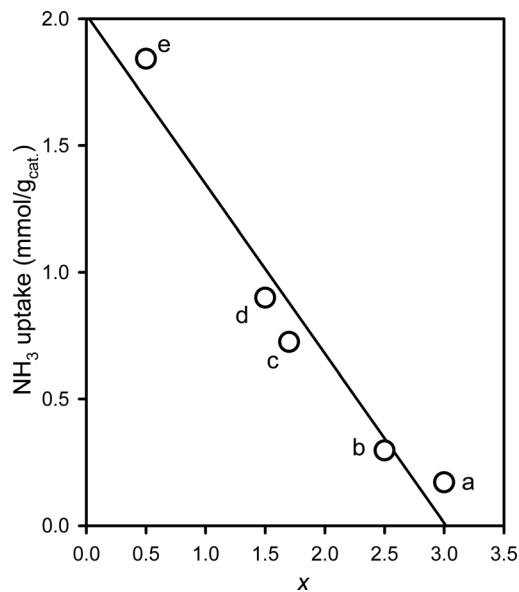


Fig. 7 Plot of the NH₃ uptake as a function of the Cs loading expressed as *x* in the Cs_{*x*}(NH₄)_{3–*x*}HPMO₁₁VO₄₀ formula [a: Cs₃(NH₄)₀H, b: Cs_{2.5}(NH₄)_{0.5}H, c: Cs_{1.7}(NH₄)_{1.3}H, d: Cs_{1.5}(NH₄)_{1.5}H, e: Cs_{0.5}(NH₄)_{2.5}H].

However the highest yield in MAC + MAA (5.5%) was obtained over the Cs_{1.7}(NH₄)_{1.3}H sample, corresponding to an isobutane conversion of 9.6% and an oxygen conversion of 52.7%. Cs_{1.7}(NH₄)_{1.3}H and Cs_{2.5}(NH₄)_{0.5}H catalysts showed similar activity in isobutane oxidation, but different product distributions were observed. In fact, whereas Cs_{1.7}(NH₄)_{1.3}H exhibited a higher selectivity to both MAC (13.7%) and MAA (43.4%), and relatively low selectivity to CO_x (25.6%), Cs_{2.5}(NH₄)_{0.5}H exhibited a very high selectivity to CO_x (53.1%). By comparing the converted reactants, it was noteworthy that Cs_{2.5}(NH₄)_{0.5}H shows very high ratio of oxygen/isobutane conversion (10/1) compared to the other samples (*ca.* 5/1). We shown in a previous study²⁶ that consecutive combustion of the desired products mainly occurs in the case of MAC, whereas MAA is rather stable under the reaction conditions. In terms of competitive reaction to convert MAC to MAA or to CO_x, Cs_{2.5}(NH₄)_{0.5}H exhibited a greater ability in promoting the degradation reaction instead of the selective oxidation to MAA. The Cs₃(NH₄)₀H sample gave the lowest activity as a consequence of the low amount of acid sites, resulting in difficulty for activating the C–H bond of isobutane.

Finally, the influence of the acidity on the catalytic activity is reported in Fig. 8. The sample Cs₃(NH₄)₀H having the

Table 3 Amount of acidic sites and strength distribution over the samples, determined from the NH₃-TPD profiles

Catalyst	Acidity, NH ₃ uptake, mmol g _{cat.} ⁻¹			Total acidity mmol g _{cat.} ⁻¹ (μmol m _{cat.} ⁻²)
	130–300 weak	300–450 medium	450–560 strong	
Cs _{0.5} (NH ₄) _{2.5} H	0.00	0.68	1.16	1.84 (317.55)
Cs _{1.5} (NH ₄) _{1.5} H	0.01	0.89	—	0.90 (107.03)
Cs _{1.7} (NH ₄) _{1.3} H	0.02	0.71	—	0.72 (44.16)
Cs _{2.5} (NH ₄) _{0.5} H	0.07	0.23	—	0.30 (5.06)
Cs ₃ (NH ₄) ₀ H	0.07	0.10	—	0.17 (1.94)

Table 4 Catalytic performances in IBAN selective oxidation^a

Catalyst	Conversion, %		Selectivity, %					$Y_{(\text{MAC}+\text{MAA})}$, %	Carbon balance
	O ₂	IBAN	MAC	AA	ACA	MAA	CO _x		
Cs ₀ (NH ₄) ₃ H (APMV)	10.4	2.0	11.5	11.9	6.2	32.9	37.5	0.9	0.992
Cs _{0.5} (NH ₄) _{2.5} H	17.1	4.1	29.3	9.3	3.1	41.5	16.8	2.9	0.995
Cs _{1.5} (NH ₄) _{1.5} H	29.2	5.8	22.1	10.7	3.3	44.8	19.1	3.9	0.997
Cs _{1.7} (NH ₄) _{1.3} H	52.7	9.6	13.7	13.4	3.9	43.4	25.6	5.5	0.997
Cs _{2.5} (NH ₄) _{0.5} H	100.0	9.9	9.7	15.5	2.6	19.1	53.1	2.9	0.998
Cs ₃ (NH ₄) ₀ H	6.2	1.2	16.2	19.9	9.0	31.9	23.0	0.6	0.996

^a Reaction conditions: temperature = 340 °C, atmospheric pressure, contact time = 4.8 s, time on stream = 18 h. Here IBAN = isobutane, MAC = methacrolein, AA = acetic acid, ACA = acrylic acid and MAA = methacrylic acid.

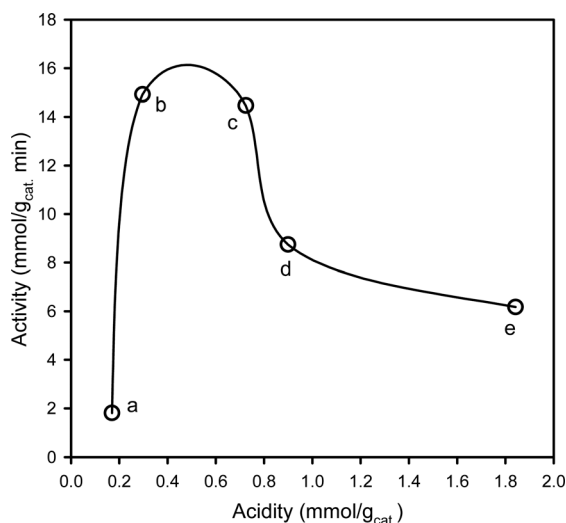


Fig. 8 Correlation between the catalytic activity and acidity [a: Cs₃(NH₄)₀H, b: Cs_{2.5}(NH₄)_{0.5}H, c: Cs_{1.7}(NH₄)_{1.3}H, d: Cs_{1.5}(NH₄)_{1.5}H, e: Cs_{0.5}(NH₄)_{2.5}H].

lowest amount of acid sites (0.17 mmol g⁻¹ NH₃ uptake) shows the lowest activity (1.81 μmol g_{cat.}⁻¹ min⁻¹). As the number of acid sites increases to 0.30 mmol g⁻¹ for Cs_{2.5}(NH₄)_{0.5}H, the activity for isobutane oxidation increase sharply to 14.92 μmol g_{cat.}⁻¹ min⁻¹. A similar value is obtained for the Cs_{1.7}(NH₄)_{1.3}H catalyst which exhibits an increased acidity of 0.72 mmol g⁻¹. On the other hand, a further increase in the number of acid sites, as for the Cs_{1.5}(NH₄)_{1.5}H and Cs_{0.5}(NH₄)_{2.5}H samples do not improve the activity anymore, which may be related to the low surface area of the samples. As a matter of fact, the selective oxidation of isobutane over heteropolycompounds catalysts was classified as a surface-type reaction.²²

It has been proved that the mechanism of isobutane oxidation involves an oxidative dehydrogenation step to give isobutene,^{27–29} which is subsequently converted to MAC and MAA, 500 times faster than it is formed. The C–H bond activation, which is therefore considered as the rate-limiting step, is promoted by the surface acidic sites.^{24,26} Activity and acidity were then accounted per unit of catalyst surface (with the notion of surface acid density discussed in a

previous work,³ and their relationship is depicted in Fig. 9. A pronounced increase in activity from 0.02 to 0.25 μmol m_{cat.}⁻² min⁻¹ can be seen as x decreases from 3 to 2.5, corresponding to an increase in surface acid density from 1.9 to 5.1 μmol m_{cat.}⁻² (points labelled 'a' and 'b' on the figure). Then, the activity continues to increase to 0.88 μmol m_{cat.}⁻² min⁻¹ when x further decreases to 1.7, although the slope becomes a little bit less pronounced. Further, the activity still increases, but with a quite slow slope until it reaches a plateau around 1.07 μmol m_{cat.}⁻² min⁻¹, for the low x value 0.5 with a surface acid density of 317.6 μmol m_{cat.}⁻². The sharp increase in activity from Cs₃(NH₄)₀H to Cs_{2.5}(NH₄)_{0.5}H indicates the importance of the acidic sites in the activation step. However, it is not the unique important factor that governs the catalytic performances, since the quite low surface area also restricted the conversion of isobutane, as observed over Cs_{1.5}(NH₄)_{1.5}H and Cs_{0.5}(NH₄)_{2.5}H catalysts, despite the fact that they possess a relatively high number of acid sites. The highest activity is obtained neither over the catalyst with the strongest acidity (labelled e in Fig. 9) nor over the catalyst with largest specific surface area (labelled a in Fig. 9). Since the specific surface area and the acidity show an opposite trend when varying the Cs loading (and, thus

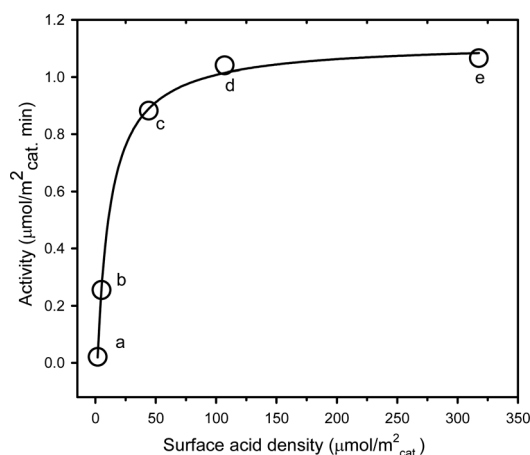


Fig. 9 Relationship between the activity and the surface acid density [a: Cs₃(NH₄)₀H, b: Cs_{2.5}(NH₄)_{0.5}H, c: Cs_{1.7}(NH₄)_{1.3}H, d: Cs_{1.5}(NH₄)_{1.5}H, e: Cs_{0.5}(NH₄)_{2.5}H].

when varying x), it then become crucial to find the “key point” in order to gain the appropriate acidity and surface area, which ensures high isobutane conversion. According to our results, the optimum is then between 1.7 and 2.5 Cs atom per Keggin unit.

4. Conclusions

Mixed salts $\text{Cs}_x(\text{NH}_4)_{3-x}\text{HPMo}_{11}\text{VO}_{40}$ ($x = 0-3$) were prepared by the precipitation method. Their properties such as texture, nature, crystallinity and acidity were determined and successfully correlated to the Cs substitution extent represented by x in the previous formula. We suggest that the introduction of caesium in the catalysts formula stabilized the Keggin structure and limited the expelling of vanadium from the primary structure, avoiding mono-oxide phase segregation. Furthermore, the specific surface area increases with the Cs content in the catalyst. However, as a consequence of the $\text{Cs}^+/\text{NH}_4^+$ ratio increase, a decrease in the number of acid sites was concomitantly observed. This opposite trend implies that a trade-off has to be found to keep a sufficiently high acid site density, which is of main importance for the catalytic activity since the isobutane selective oxidation takes place on acid active sites at the surface of the catalyst. Thus, proper balance between acidity and specific surface area enables getting an optimised yield, which was observed over $\text{Cs}_{1.7}(\text{NH}_4)_{1.3}\text{H}$. This latter exhibited an isobutane conversion of 9.6%, and a total selectivity to the desired products MAC + MAA of 57.1%.

Acknowledgements

The authors thank O. Gardoll and G. Cambien for TG and N_2 adsorption/desorption analyses, respectively. The Fonds Européen de Développement Régional (FEDER), CNRS, Région Nord Pas-de-Calais and Ministère de l'Education Nationale de l'Enseignement Supérieur et de la Recherche are acknowledged for fundings of X-ray diffractometers. The staffs and PhD students in Ecole Centrale de Lille are also acknowledged for their kind supports. F. Jing thanks the China Scholarship Council (CSC) for providing the financial support during his stay in France.

References

- N. Mizuno and H. Yahiro, *J. Phys. Chem. B*, 1998, **102**, 437–443.
- F. Jing, B. Katryniok, E. Bordes-Richard and S. Paul, *Catal. Today*, 2013, **203**, 32–39.
- F. Jing, B. Katryniok, F. Dumeignil, E. Bordes-Richard and S. Paul, *J. Catal.*, 2014, **309**, 121–135.
- K. Inumaru, T. Ito and M. Misono, *Microporous Mesoporous Mater.*, 1998, **21**, 629–635.
- T. Okuhara, H. Watanabe, T. Nishimura, K. Inumaru and M. Misono, *Chem. Mater.*, 2000, **12**, 2230–2238.
- J. S. Santos, J. A. Dias, S. C. L. Dias, F. A. C. Garcia, J. L. Macedo, F. S. G. Sousa and L. S. Almeida, *Appl. Catal., A*, 2011, **394**, 138–148.
- C. Marchal-Roch, N. Laronze, R. Villanneau, N. Guillou, A. Tézé and G. Hervé, *J. Catal.*, 2000, **190**, 173–181.
- J. He, H. Pang, W. Wang, Y. Zhang, B. Yan, X. Li, S. Li and J. Chen, *Dalton Trans.*, 2013, **42**, 15637–15644.
- T. Ressler, U. Dorn, A. Walter, S. Schwarz and A. H. P. Hahn, *J. Catal.*, 2010, **275**, 1–10.
- P. Visuvamithiran, K. Shanthi, M. Palanichamy and V. Murugesan, *Catal. Sci. Technol.*, 2013, **3**, 2340–2348.
- T. Okuhara, H. Watanabe, T. Nishimura, K. Inumaru and M. Misono, *Chem. Mater.*, 2000, **12**, 2230–2238.
- F. Jing, Y. Zhang, S. Luo, W. Chu, H. Zhang and X. Shi, *J. Chem. Sci.*, 2010, **122**, 621–630.
- I. Kozhevnikov, *J. Mol. Catal. A: Chem.*, 2009, **305**, 104–111.
- I. V. Kozhevnikov, *J. Mol. Catal. A: Chem.*, 2007, **262**, 86–92.
- X.-K. Li, J. Zhao, W.-J. Ji, Z.-B. Zhang, Y. Chen, C.-T. Au, S. Han and H. Hibst, *J. Catal.*, 2006, **237**, 58–66.
- M. Sultan, S. Paul, M. Fournier and D. Vanhove, *Appl. Catal., A*, 2004, **259**, 141–152.
- C. Knapp, T. Ui, K. Nagai and N. Mizuno, *Catal. Today*, 2001, **71**, 111–119.
- C. Rocchiccioli-Deltcheff and M. Fournier, *J. Chem. Soc., Faraday Trans.*, 1991, **87**, 3913–3920.
- N. Mizuno, D. J. Suh, W. Han and T. Kudo, *J. Mol. Catal. A: Chem.*, 1996, **114**, 309–317.
- N. Ballarini, F. Candiracci, F. Cavani, H. Degrand, J. L. Dubois, G. Lucarelli, M. Margotti, A. Patinet, A. Pigamo and F. Trifiro, *Appl. Catal., A*, 2007, **325**, 263–269.
- C. Marchal-Roch, C. Julien, J. F. Moisan, N. Leclerc-Laronze, F. X. Liu and G. Herve, *Appl. Catal., A*, 2004, **278**, 123–132.
- N. Mizuno, M. Tateishi and M. Iwamoto, *J. Catal.*, 1996, **163**, 87–94.
- F. Cavani, *Catal. Today*, 1998, **41**, 73–86.
- G. Busca, F. Cavani, E. Etienne, E. Finocchio, A. Galli, G. Sella and F. Trifiro, *J. Mol. Catal. A: Chem.*, 1996, **114**, 343–359.
- N. Mizuno and M. Misono, *Chem. Rev.*, 1998, **98**, 199–217.
- S. Paul, V. LeCourtois and D. Vanhove, *Ind. Eng. Chem. Res.*, 1997, **36**, 3391–3399.
- Q. Huynh, Y. Schuurman, R. Delichere, S. Loidant and J. M. M. Millet, *J. Catal.*, 2009, **261**, 166–176.
- G. P. Schindler, T. Ui and K. Nagai, *Appl. Catal., A*, 2001, **206**, 183–195.
- L. Jalowiecki-Duhamel, A. Monnier, Y. Barbaux and G. Hecquet, *Catal. Today*, 1996, **32**, 237–241.